Positron Imaging of Myocardial Infarction with Rubidium-82

Richard A. Goldstein, Nizar A. Mullani, Wai-Hoi Wong, Ross K. Hartz, Charles H. Hicks, Francisco Fuentes, Richard W. Smalling, and K. Lance Gould

Division of Cardiology, Positron Diagnostic and Research Center, The University of Texas Medical School at Houston, Houston, Texas

Positron imaging provides tomographic images of regional myocardial perfusion but has required an on-site cyclotron. Rubidium-82 (^{82}Rb) is a short-lived ($T_{½}$ = 75 sec) positron emitter available from a generator. In order to determine the feasibility for its use to image acute myocardial infarction, 18 patients with transmural infarctions who had coronary arteriography were given 30–40 mCi of ^{82}Rb intravenously and positron tomographic imaging was carried out within 96 hr after onset of symptoms. Nine simultaneous transaxial slices were obtained for each patient with a positron camera. Images were also reconstructed in a long-axis, short-axis, and three-dimensional display. One study could not be interpreted because of excessive lung activity. Fourteen normals were also studied. The infarct related artery determined by angiography was correctly diagnosed by positron imaging in all 17 patients as were all three prior infarcts by readers blinded to the clinical data. No defects were observed in normals or in noninfarcted myocardial regions. This study indicates that ^{82}Rb should be useful for perfusion imaging in patients with acute myocardial infarction. The short half-life of ^{82}Rb should make it ideal for providing serial assessment of perfusion in patients undergoing thrombolytic therapy.

J Nucl Med 27:1824–1829, 1986

Several single photon emitting tracers have been used for qualitative imaging of patients with acute myocardial infarction (*1*). The physical properties of these tracers, however, preclude quantification and their long half-lives limit them to a single study for evaluating an infarction undergoing continual evolution. Positron emitters obviate the attenuation problems inherent in the use of single photon emitters since quantification can be achieved using coincidence methods with positron tomographic reconstruction (*2*). Furthermore, positron emitters have a short half-life allowing serial imaging.

Rubidium-82 (^{82}Rb) is a positron emitting potassium analog ($T_{½}$ = 75 sec) that can be obtained from a desktop generator system with a shelf-life of 4–6 wk. Initial studies have demonstrated that images with ^{82}Rb can be used to diagnose coronary artery disease (*3–5*). We have previously demonstrated that time-activity curves of ^{82}Rb can be used to assess coronary artery patency and viability of myocardium at risk under experimental conditions (*6*). The purpose of the current study was to determine whether qualitative positron imaging of myocardial infarction is clinically feasible using a generator produced positron emitter.

Received Dec. 11, 1985; revision accepted June 12, 1986.

For reprints contact: Richard A. Goldstein, MD, Director, Nuclear Cardiology, University of Texas Medical School, P.O. Box 20708, Houston, TX 77225-0708.

PATIENTS AND METHODS

Study Population

The study group included 18 patients with acute myocardial infarction and 14 control patients. The group of patients with infarction consisted of 16 men and two women with ages ranging from 34–79 yr (mean 52.4). All infarct patients presented to the emergency room or coronary care unit and underwent positron imaging within 96 hr of the onset of chest pain. Infarction was documented by a history of typical chest pain, acute ST changes with evolution of Q waves on electrocardiography and serial changes in plasma MB creatine kinase activity. Total creatine kinase activity averaged 1,928 ± 1,557 (s.d.) I.U. (range 279 – 5,580) and CK – MB averaged 207 ± 231 I.U. (range 4 – 970). Cardiac catheterization and coronary arteriography was performed within 24 hr of imaging. The control group consisted of six men and eight women ages 28–59 yr

(mean 45.2) who had diagnostic coronary angiography for evaluation of chest pain but had normal coronary anatomy (n = 11) or had a normal treadmill stress test with thallium-201 (^{201}Tl) (n = 3).

Imaging Protocol

Each patient was positioned in multislice positron tomographic camera (TOFPET I) such that the entire heart was within nine simultaneous transverse image planes. The patient position was marked using a laser light source. The camera consists of 720 cesium fluoride detectors grouped in five rings of 144 detectors each (*7*). The system wobbles every second for improved resolution. Although data was collected in a list mode that is gated to the EKG, nongated images were used for interpretation. The intrinsic geometric resolution of the detectors has been measured at 8.1 mm full width at half maximum (FWHM). The reconstructed resolution of 11 mm FWHM is used for clinical studies.

After positioning, a transmission scan was performed using a Plexiglas ring containing 3 mCi of gallium-68 (^{68}Ga) to correct for tissue attenuation. Each transmission scan contained ~80 million coincidence events for all nine slices. The ring was then removed, the positioning re-checked, and 30 or 40 mCi of ^{82}Rb from a ^{82}Sr/^{82}Rb generator were infused intravenously (*8*). The infusion device allows the operator to set limits for total dose, dose rate, and delivered volume. Data collection was started 1 min after the end of infusion. The total coincidence count rate at the start of data collection was typically 200,000 cps and singles count rate was 20,000 cps per detector. The coincidence timing window is set at 10 nsec for a true to random rate of 1:1 for total counts at the start of data collection. The true to random ratio over the heart is ~10:1. An average of 19.9 ± 4.7 million coincidence counts were obtained during the 6–8 min of imaging (~2 million counts per transverse slice). Lead II of an electrocardiogram and blood pressure were monitored throughout the study period.

Data Analysis

Attenuation corrected images of ^{82}Rb uptake were reconstructed and displayed in nine transverse image planes. Time-of-flight reconstruction was not employed due to the longer processing time required for reconstruction. Long-axis (sagittal plane), short-axis (coronal plane), and three-dimensional displays of myocardial uptake of ^{82}Rb were mathematically recovered from the nine slices, as previously described (*9*). Briefly, three-dimensional reconstructions were performed by first interpolating the nine transaxial slices to 32 images and then rotating the images along two axes 30–40° to produce short-axis views (*9*). Long-axis views could then be obtained by rotating the short-axis images perpendicular to the short axis. Surface three-dimensional images were obtained from the short-axis views by representing the radial line integrals of perfusion data from the center of the ventricle to the surface of the epicardial boundary. These slices are then stacked in three dimensions and viewed from different angles as surfaces of the heart. A simpler reconstruction that represents a "pseudo-long axis" view could also be obtained by selecting data along the axial direction from the interpolated slices (Figs. 1A and 1B). A similar approach can be used to obtain a "pseudo-short axis" view (Figs. 1C and 1D). Since fewer computations are required for this transformation, the interpreter can interactively choose any angle or regions to be viewed within a few seconds.

Data in the images were presented in a color coded scale and regional pixel values were interactively available for reading the relative concentration of ^{82}Rb in the myocardium and for obtaining the ratio of uptake in the normal myocardium to the uptake in the infarcted regions. In the 9-slice transaxial reconstruction, colors are assigned on a 256 scale with areas of greatest activity presented in white followed by red, yellow, green, etc., through the spectrum. Each drop in color corresponds to a 15% decrease in counts. The color of normal segments of the heart will be dependent on other activity within the nine slices. For example, if slice nine contains the kidney which concentrates ^{82}Rb, the *relative* counts in the heart will be less and the color scaled down accordingly. In general, perfusion defects were considered to be present if there was a one-step difference in counts from a normal area on two contiguous slices.

Positron tomographic images were interpreted independently by two investigators blinded to the clinical data. In cases with less than complete agreement, studies were reviewed again for a consensus interpretation. The infarct related coronary artery was determined by angiography. The positron emission tomographic (PET) image and coronary angiogram were considered to be in agreement as follows: a left anterior descending coronary occlusion corresponded to a defect in anterior and/or septal regions, a left circumflex occlusion to a lateral-posterior defect, and a right coronary occlusion to an inferior-posterior defect.

RESULTS

The blood pressure and cardiac rhythm remained stable in all patients during the imaging periods. One patient developed chest pain during the transmission image acquisition and was treated with nitroglycerin.

Controls

A representative set of transverse images from a normal patient is shown in Fig. 1A. In this figure, images are presented left to right from the base of the heart (in the upper left) to the apex (at the lower left).

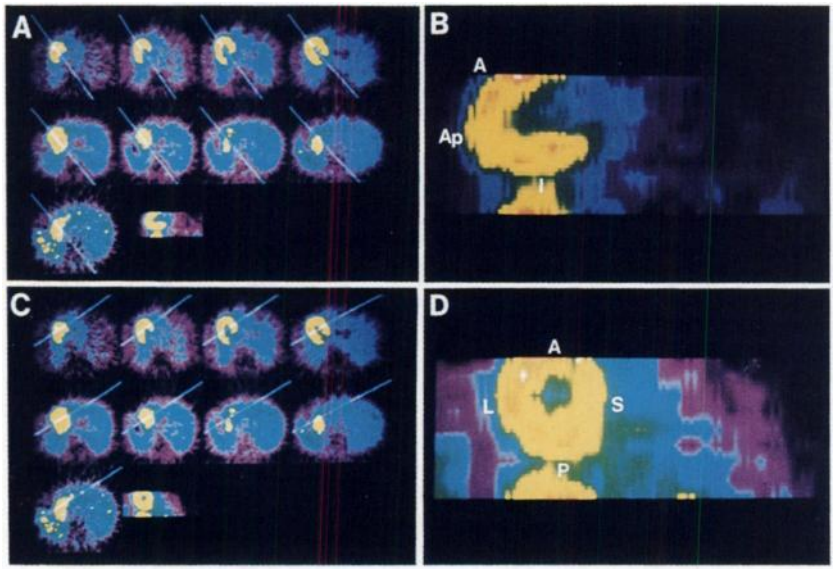

FIGURE 1
Normal ^{82}Rb perfusion images. A: Nine simultaneous transaxial ^{82}Rb emission slices from normal patient. Images are oriented from base of heart on upper left of nine slices to apex at lower left. No perfusion defects were present. Lines drawn through each image represent data selected for "pseudo-long axis" view which is then shown at lower right of figure and enlarged in B. C: Nine slice orientation is same as A except that lines illustrate data chosen for "pseudo-short axis." D: Enlarged "pseudo-short axis" view from C. Ap = Apical; I = Inferior; P = Posterior; S = Septal

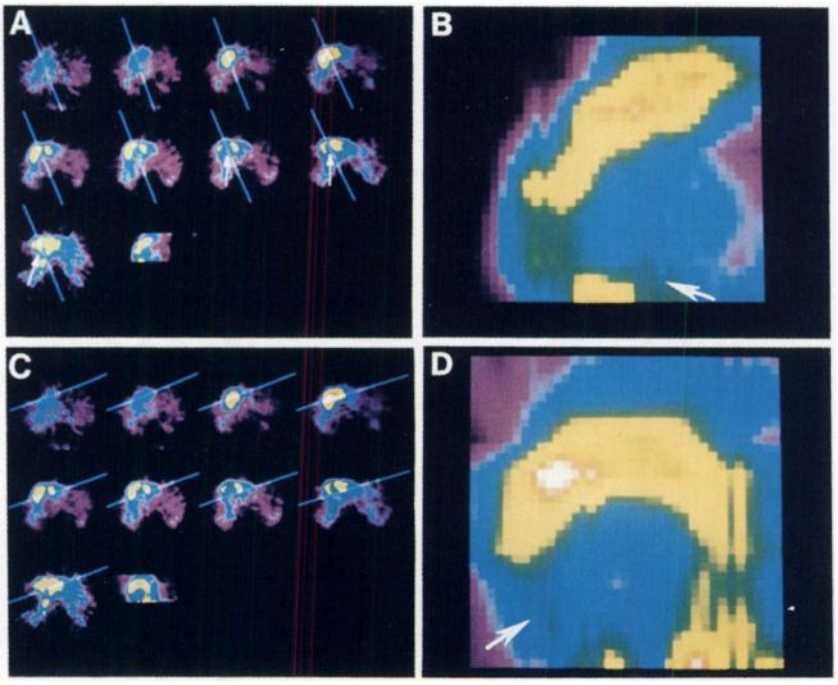

FIGURE 2
Rubidium-82 perfusion images from patient with occlusion of left circumflex coronary artery. Orientation is same as in Fig 1. Arrows point to posterior-lateral defects

The left of the image corresponds to the left of the patient. This presentation differs from the conventional tomographic displays, but has the advantage of allowing the interpreter to view the images as if he is looking down on his own chest for easier anatomic orientation. Figures 1B and 1D present a "pseudo-long axis" and "pseudo-short axis" view, respectively. There were no areas of abnormal perfusion in the 14 control patients (Table 1).

Infarct Patients

The 18 infarct patients had a total of 21 occluded arteries. In the three cases of multiple occlusions, the acute infarct was considered to be the artery with concordant ST segment elevation on the electrocardiogram and/or appearance of acute thrombosis by arteriography. All nine patients with occlusions of the left anterior descending coronary artery (eight acute, one remote) had anterior and/or septal defects. Two patients with acute left circumflex coronary occlusions and one patient with a previous circumflex occlusion had lateral-posterior defects (Figs. 2 and 3). In eight patients with acute right coronary occlusion, seven had inferior defects (Figs. 4 and 5); images from the other patient were considered uninterpretable because of ex-

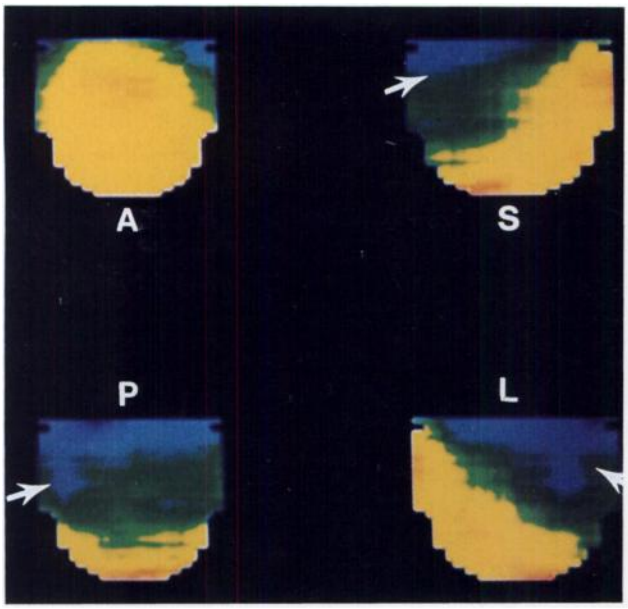

FIGURE 3
Three-dimensional perfusion images in patient with occlusion of left circumflex coronary artery. In this format, multiple short axis images are stacked such that transmural activity is presented in thin shell viewed as external surfaces of heart. Patient is same as in Fig 2. Arrow points to large posterior-lateral perfusion defect

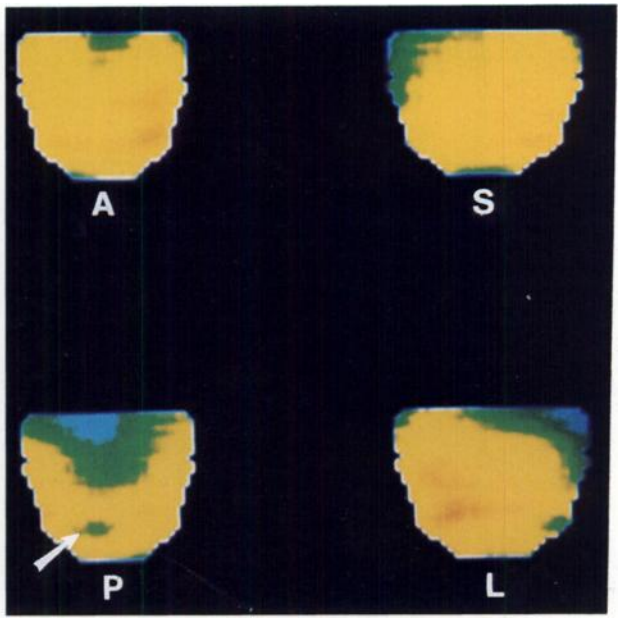

FIGURE 5
Three-dimensional perfusion images in patient with right coronary artery occlusion. Patient is same as in Fig 4. Arrow points to small posterior perfusion defect that was not readily apparent on transaxial or short axis slices because of size of defect

cessive lung activity which also precluded interpretation of planar ^{201}Tl images. A remote right coronary occlusion was also associated with an inferior defect in a patient with an acute LAD occlusion and an anterior defect on PET.

DISCUSSION

Clinical imaging of regional myocardial perfusion in patients with acute myocardial infarction has not routinely been used in most hospitals since the diagnosis can usually be made on the basis of the clinical history, electrocardiogram, and serial cardiac isoenzymes. Since left ventricular function and survival may improve following successful thrombolytic therapy with streptokinase and tissue plasminogen activating factor, there is need for a short-lived tracer to size the infarct repeatedly and follow the effect of treatment (*10*, *11*). Washout curves of ^{201}Tl can be used to determine tissue viability in experimental models of infarction (*12*, *13*).

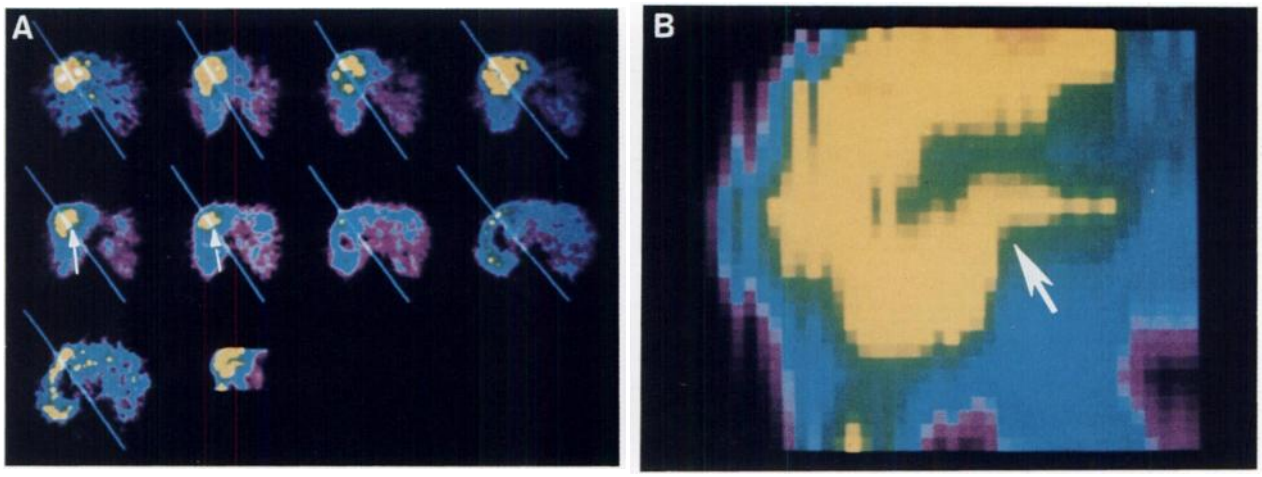

FIGURE 4
Rubidium-82 perfusion images from patient with occlusion of right coronary artery. Orientation is same as in Figs 1A and B. Arrows in A point to small posterior defect and in B an inferior defect

TABLE 1
PET Imaging in Acute Myocardial Infarction*

Rb perfusion defect	Infarct related artery				
	LAD	LCX	RCA	None	Total
A-S	8 (1)	0	0	0	8 (1)
L-P	0	2 (1)	0	0	2 (1)
I-P	0	0	7 (1)	0	7 (1)
None	0	0	0	14	14
Inadequate	0	0	1	0	1
Total	8 (1)	2 (1)	8 (1)	14	32 (3)

*Figures refer to number of patients. Figures in parenthesis represent patients with remote infarctions. A = Anterior; S = Septal; L = Lateral; I = Inferior; P = Posterior; LAD = Left anterior descending coronary artery; LCX = Left circumflex coronary artery; RCA = Right coronary artery.

The time interval between initial perfusion and redistribution images (2–4 hr), however, is not short enough to be useful as an index of viability in evolving myocardial infarctions.

Rubidium-82 has physical characteristics that are ideal for acute infarct imaging including its 75-sec half-life that allows repetitive imaging as often as every 10 min. The tracer is administered directly from an infusion system which contains an intrinsic radiation monitoring-feedback-control system and does not require any additional chemical processing. The use of ^{82}Rb as a myocardial perfusion indicator has been validated in animal models using beta radiation detectors (*14, 15*). Two mathematic models have been developed to measure flow *per se* with ^{82}Rb but require arterial sampling and extensive data computation (*14–17*). However, since uptake of ^{82}Rb is linearly related to flows from 0 to 1.5 times normal resting flow, images of ^{82}Rb uptake represent a much simpler approach for assessment of perfusion deficits due to myocardial infarction. In open-chested dogs, ^{82}Rb time-activity curves can be used to assess the functional integrity of the myocardial cell membrane (*6*). The net rate constant for ^{82}Rb transfer after delivery of the tracer (corrected for physical decay) is positive in normal and potentially viable myocardium, whereas tissue that is irreversibly injured after reperfusion has a negative rate constant indicating tracer leakage. The failure to increase extraction with low flows of ^{82}Rb may be an early harbinger of loss of viability (*18*). Similar approaches in man should provide significant information about preservation of myocardium following thrombolysis, in addition to the determination of artery patency.

This study presents our initial clinical experience with three-dimensional surface images of the heart. Traditionally, positron images of the myocardium have been displayed as transverse slices. However, this presentation is limited for visualization of the inferior wall abnormalities. Single photon emission tomographic (SPECT) ^{201}Tl images are commonly reconstructed in short- and long-axis views in order to obviate this problem. Integration of multislice information by the interpreter, however, may be difficult for routine analysis. Several investigators have described a "bullseye" presentation for SPECT images that consists of a central apical short-axis slice with rings of superior short-axis slices added concentrically (*19*). Although initial results with this format are encouraging, problems of attenuation from breast and adipose tissue remains a problem for SPECT. In the current study, attenuation corrected images were reconstructed in the short axis view and stacked into a true three-dimensional image that can be displayed on a computer monitor by rotating the image such that anterior, lateral, posterior, and septal aspects of the heart can be visualized for relative size and location of defects. At present, the three-dimensional approach provides qualitative displays. A quantitative three-dimensional display based on these reconstructions is currently under investigation.

The current study demonstrates the clinical feasibility of three dimensional positron imaging after i.v. ^{82}Rb in acute infarction. Regions of hypoperfusion correspond to the artery occluded at coronary angiography. Additional studies are needed in order to define the quantitative value of this approach for determining arterial patency, infarct size, and myocardial viability in man.

ACKNOWLEDGMENTS

The authors thank Janice Kuhn, RN, Margaret Matthews, RN, Mark Wilson, Keith Yerian, Jay Gaeta, and M. V. Ranganath for their assistance. This work was supported in part by grants from the NIH (Grant 2RO1 H126862-D4), the American Heart Association, and contract DE-FG05-84ER60210, U.S. Department of Energy.

The ^{82}Rb generator was provided by Squibb Diagnostics courtesy of Michael D. Loberg, PhD, Meg Graff, Michael Swiatochia, and Marion Meeks, PhD. This work was carried out as a joint collaborative research project with the Clayton Foundation for Research, Houston, TX.

REFERENCES

1. Wackers FJTh, Sokole EB, Samson G, et al: Value and limitations of thallium-201 scintigraphy in the acute phase of myocardial infarction. *N Engl J Med* 295:1–5, 1976
2. Goldstein RA, Mullani NA, Gould KL: Quantitative Myocardial Imaging with Positron Emitters. In *Progress in Cardiology*, Vol 12, Yu PN, Goodwin JF, eds. Philadelphia, Lea and Febiger, 1983
3. Deanfield JE, Kensett M, Wilson RA, et al: Silent myocardial ischemia. *Lancet* 2:1001, 1984
4. Deanfield JE, Shea M, Ribiero P, et al: Transient ST-segment depression as a marker of myocardial ischemia during daily life. *Am J Cardiol* 54:1195–1200, 1984

5. Gould KL, Goldstein RA, Mullani NA, et al: Noninvasive assessment of coronary stenoses by myocardial perfusion imaging during pharmacologic vasodilation. VIII. Clinical feasibility of positron cardiac imaging without a cyclotron using rubidium-82. *JACC* 7:775–789, 1986
6. Goldstein RA: Kinetics of rubidium-82 after coronary occlusion and reperfusion: Assessment of patency and viability in open-chested dogs. *J Clin Invest* 75:1131–1137, 1985
7. Mullani NA, Gaeta J, Yerian K, et al: Dynamic Imaging with High Resolution Time-of-Flight PET Camera—TOFPET I. *IEEE Trans Nucl Sci* S-31, No. 1, 609–613, 1984
8. Neirinckx RD, Kronauge JF, Gennaro GP, et al: Evaluation of inorganic absorbents for rubidium-82 generator: I. Hydrous SnO_2. *J Nucl Med* 24:898–906, 1982
9. Kehtarnavaz N, Philippe EA, DeFigueiredo RJP: An oval surface reconstruction and display method for cardiac PET images. *IEEE Trans Med Imag* MI-3:108–115, 1984
10. Kennedy JW, Ritchie JL, David KB, et al: Western Washington Randomized trial of intracoronary streptokinase in acute myocardial infarction. *N Engl Med* 309:1477–1482, 1983
11. Smalling RW, Fuentes F, Matthews MW, et al: Sustained improvement in left ventricular function and mortality by intracoronary streptokinase administration during evolving myocardial infarction. *Circulation* 68:131–138, 1983
12. Okada RD, Pohost GM: The use of preintervention and postintervention thallium imaging for assessing the early and late effects of experimental coronary arterial reperfusion in dogs. *Circulation* 69:1153–1160, 1984
13. Okada RD: Kinetics of thallium-201 in reperfused canine myocardium after coronary occlusion. *JACC* 3:1245–1251, 1984
14. Mullani NA, Gould KL: First pass regional blood flow measurements with external detectors. *J Nucl Med* 24:577–581, 1983
15. Mullani NA, Goldstein RA, Gould KL, et al: Myocardial perfusion with rubidium-82: I. Measurement of extraction fraction and flow with external detectors. *J Nucl Med* 24:898–906, 1983
16. Goldstein RA, Mullani NA, Fisher DJ, et al: Myocardial perfusion with rubidium-82: II. Effects of metabolic and pharmaceutical interventions. *J Nucl Med* 24:907–915, 1983
17. Mullani NA: Myocardial perfusion with rubidium-82: III. Theoretical basis for relating quantitative perfusion to severity of coronary stenosis. *J Nucl Med* 25:1190–1196, 1984
18. Goldstein RA: Rubidium-82 kinetics after coronary occlusion: Temporal relation of net myocardial accumulation and viability in open-chested dogs. *J Nucl Med* 27:1456–1461, 1986
19. Caldwell JH, Williams DC, Harp GD, et al: Quantification of site of relative myocardial perfusion defect by single photon emission computed tomography. *Circulation* 70:1048–1056, 1984